Appl. Phys. B (2013) 113:463–471
DOI 10.1007/s00340-013-5491-5

Applied Physics B
Lasers and Optics

Solvent-related effects in MAPLE mechanism

A. P. Caricato · V. Arima · M. Cesaria · M. Martino · T. Tunno · R. Rinaldi · A. Zacheo

Received: 31 July 2012 / Accepted: 14 December 2012

Abstract To study the role of the solvent and of the laser fluence in the matrix-assisted pulsed laser evaporation (MAPLE) process, we used a soft polymer (polydimethylsiloxane—PDMS) as "sensing surface" and toluene as solvent. Thin films of the PDMS polymer were placed in the position of the growing film, while a frozen toluene target was irradiated with an ArF laser at the conventional fluences used in MAPLE depositions (60–250 mJ/cm^2). Apart the absence of solute, the MAPLE typical experimental conditions for the deposition of thin organic layers were tested. The effects on the PDMS films of the toluene target ablation, at different fluences, were studied using atomic force microscopy and contact angles measurements. The results were compared with the effects produced on similar PDMS films by four different treatments (exposure to a drop of the solvent, to saturated toluene vapors and to plasma sources of two different powers). From this comparative study, it appears that depending on the MAPLE experimental conditions: (1) the MAPLE process may be "semidry" rather than purely dry (namely the solvent is likely to be present in the deposition environment near the growing film), (2) the solvent, if sufficiently volatile, is in form of vapor molecules (neutral, ionized and probably dissociated) rather than in liquid phase near the substrate and (3) at relatively high laser fluences (>150 mJ/cm^2), the formation of an intense plasma plume results which can damage/affect a soft substrate as well as a growing polymer film.

A. P. Caricato (✉) · M. Cesaria · M. Martino · T. Tunno · R. Rinaldi · A. Zacheo
Department of Mathematics and Physics "E. De Giorgi", University of Salento, Via Arnesano, 73100 Lecce, Italy
e-mail: annapaola.caricato@le.infn.it

V. Arima · R. Rinaldi · A. Zacheo
National Nanotechnology Laboratory (NNL), Istituto Nanoscienze-CNR, Via Arnesano n. 16, 73100 Lecce, Italy

1 Introduction

There is a growing interest about polymeric thin films and nanostructures for their perspective applications in realizing new and high-performance devices [1–3]. The deposition of polymers and biomaterials in form of thin films, multilayers and composite structures is not an easy task, since the structural, morphological, and chemical composition of the materials must be fully maintained to preserve their properties. Even stronger requirements must be satisfied on film uniformity, thickness control and interface properties in the case of deposition of multilayers [4–6].

Thin films of polymers are normally prepared by solvent-based methods, such as spin coating, dip coating and drop casting, which are quick and inexpensive but do not allow a fine control of the surface and sufficient thickness homogeneity of the deposits. For this purpose, in the last years, laser-based techniques were extensively studied and tested. However, the results suggest that much work is necessary to find the best way of creating polymer films [7].

Pulsed laser depositions (PLD) of polymers were reported by Srinivasan et al. [8] and Kawamura et al. [9] already in 1982. Thereafter, a number of research papers and reviews on laser ablation of a large variety of polymers have been published [10–18]. From these papers, it results that very few polymers can be efficiently deposited by using this technique.

A modified PLD approach, more suitable for soft materials deposition, was introduced, the matrix-assisted pulsed laser evaporation (MAPLE) technique [19]. Here, the material of interest is dissolved or suspended in a

volatile solvent with a typical concentration of a few weight percent. The resulting solution is then frozen at the liquid nitrogen (LN_2) temperature, forming the target to be laser-irradiated. The laser energy is mainly absorbed by the solvent, which vaporizes, thereby entangling the solute material and promoting its deposition onto the desired substrates. Since the laser energy is principally absorbed by the volatile solvent, lower energy densities (typically tens of mJ/cm^2) with respect to PLD are used, thus allowing the laser–solute interaction to be minimized.

The MAPLE technique has been successfully used for the deposition of different kinds of polymer materials, proteins and bioactive materials [20–23]. Recently, it was successfully used for the deposition of polymer blends and composite materials [24, 25]. PMMA films deposited by the MAPLE technique exhibited particular interesting properties compared to those presented by the same polymer deposited with conventional techniques [26].

Moreover, very recently, the MAPLE technique was considered for the deposition of bilayer and multilayer structures [27–31], with the aim of overcoming the inherent problems connected with conventional deposition techniques, where the underlying layer can be damaged/dissolved by deposition of the overlying layer. In fact, dealing with a bilayer structure, MAPLE enables to exploit the same solvent for both layers and to accomplish a single-step MAPLE deposition [31].

However, despite the MAPLE widespread applications, the physical processes involved in the working principle are still not well understood. In this respect, dynamics and vaporization of the solvent are key points both at fundamental and applicative level.

The aim of the present work is to study the role of the solvent in the MAPLE mechanism, namely once ejected from the condensed phase due to the ablation process, apart the trivial consideration that it must dissolve the solute to be deposited and absorb the laser radiation. To this end, we considered a "sensing surface" to evaluate the eventual presence and physical state of the solvent after its ejection from the condensed phase, using experimental conditions very similar to the conventional MAPLE ones. The role of the sensing material has been played by a soft polymer, polydimethylsiloxane (PDMS), which was chosen because it is dissolved by the exploited solvent, toluene [32]. Toluene is one of the most used solvent in MAPLE experiments. Even if solute is disregarded in our study, its presence should not dramatically change the scenario because of the high solvent/solute concentration ratio in the MAPLE frozen target of any MAPLE deposition.

For each test, the PDMS film was placed in the conventional substrate position in front of the target. The frozen (LN_2 temperature) toluene targets were irradiated at different laser fluences since it is well known, from PLD tests, that the composition of the laser-produced plasma plume and the energy of the ablated specie strongly depend on the laser wavelength and laser-pulse energy density [33].

The effects on surface morphology and wettability properties were analyzed by atomic force microscopy (AFM) and contact angle (CA) measurements and correlated with the behavior of the solvent after the phase change upon laser irradiation. The results were compared with the effects induced by four different treatments (exposure to a drop of the solvent to investigate the effect of liquid toluene on PDMS, to saturated toluene vapors and to oxygen plasma sources of two different powers). The comparative study here presented seems to support the picture that a "semidry process," based on plasma-like energetic vapors may occur during MAPLE depositions.

2 Experimental apparatus and procedure

2.1 Samples $PDMS_{60}$, $PDMS_{100}$, $PDMS_{150}$, $PDMS_{200}$ and $PDMS_{250}$

Ten μm thick PDMS films were prepared by spin coating of a PDMS solution in toluene (4:1 weight ratio) on 2 cm × 2 cm Si wafers. The films were then baked at 140 °C for 15 min to achieve thermal crosslinking.

Commercial PDMS material from Dow Corning (Sylgard 184, available as a two-component kit) was used. It consists of a base (liquid silicone rubber) and a curing agent (mixture of platinum complex and copolymers of methylhydrosiloxane and dimethylsiloxane). The base and the curing agent were mixed (weight ratio of 10:1) and degassed in a sonicator. The as-prepared PDMS samples will be hereafter referred to as PDMS.

The so realized PDMS samples were placed at the usual substrate position for MAPLE depositions in front of the target at a distance of 6 cm. The target was pure toluene frozen at the LN_2 temperature (77 K). The target was inserted in the LN_2 refrigerated target holder inside a vacuum chamber, which was evacuated down to 5×10^{-4} Pa. Target rotation at 0.3 Hz was allowed during the deposition to avoid fast drilling. The irradiations were performed using 10,000 pulses generated by an ArF excimer laser ($\lambda = 193$ nm, $\tau = 20$ ns, pulse rate = 10 Hz) at the fluence (F) of 60, 100, 150, 200 and 250 mJ/cm^2, which are in the range of the used values in MAPLE experiments. These MAPLE-treated samples will be named $PDMS_{60}$, $PDMS_{100}$, $PDMS_{150}$, $PDMS_{200}$ and $PDMS_{250}$, respectively.

2.2 Samples $PDMS_v$, $PDMS_l$, $PDMS_{pl1}$ and $PDMS_{pl2}$

To evaluate the superficial modifications that toluene in different physical states may induce on PDMS upper layers,

we produced four samples: (a) a sample treated with saturated toluene vapors (named $PDMS_v$), (b) a sample treated with a toluene drop ($PDMS_l$) and (c) two samples treated with oxygen plasma ($PDMS_{pl1}$ and $PDMS_{pl2}$, respectively).

$PDMS_v$ samples After their preparation, PDMS samples were exposed overnight to toluene vapors in a saturated environment.

$PDMS_l$ samples After their preparation, PDMS samples were treated with a 1 µl toluene drop and left under hood until complete evaporation.

$PDMS_{pl1}$ samples After their preparation, PDMS samples were introduced into a commercial atmospheric plasma generator (Diener, Pico, low pressure plasma system) to induce oxygen plasma (at 50 W for 15 min).

$PDMS_{pl2}$ samples After their preparation, PDMS samples were introduced into a reactive ion etching machine (R.I.E., Ionvac) to induce oxygen plasma (at 300 W for 15 min).

In Table 1, all the accomplished surface treatments are listed.

2.3 Atomic force microscopy and contact angle characterizations

Atomic force microscopy (AFM) was used to study the morphological variation of all the PDMS previously described samples (Sects. 2.1, 2.2). AFM measurements were performed in tapping mode (Nanoscope IIIA, Veeco, USA) at room temperature in air environment. Silicon cantilevers (model *RFESPA*) with a tip radius of 8 nm, a spring constant $K = 5$ Nm^{-1} and a resonance frequency of 70–85 kHz were used. AFM was also used to quantify roughness: the reported root-mean-square (RMS) roughness values were calculated over a 228 μm^2 area, far from cracks and holes. The reported values are an average over ten measurements. The error indicates the standard deviation. Optical images of the samples were also acquired with the camera mounted on the AFM.

The effect of surface modifications on the wettability properties was investigated by water CA measurements. Static water CAs were measured using the sessile drop method and a CAM 200 instrument (KSV Instruments Ltd., Finland). The volume of the applied droplets of distilled water was 3 µl, to avoid the gravity effect on the droplet shape. The CAs listed in this work correspond to an average over four measurements performed in different parts of the sample surface, and the quoted uncertainty corresponds to the standard deviation.

Table 1 RMS surface roughness values of as-deposited PDMS film and PDMS film exposed to different treatments: toluene saturated vapors ($PDMS_v$), toluene laser-induced irradiation products at different laser fluences ($PDMS_{60}$, $PDMS_{100}$, $PDMS_{150}$, $PDMS_{200}$ and $PDMS_{250}$), soft oxygen plasma ($PDMS_{pl1}$), energetic oxygen plasma ($PDMS_{pl2}$) and liquid toluene ($PDMS_l$)

Sample name	Sample treatment	RMS (nm)
PDMS	As-deposited	6.1 ± 0.8
$PDMS_v$	Saturated toluene vapors	12.3 ± 1.5
$PDMS_{60}$	Laser ejected products at 60 mJ/cm^2	53 ± 3
$PDMS_{100a}$	Laser ejected products at 100 mJ/cm^2 (peripheral zone)	105 ± 14
$PDMS_{100b}$	Laser ejected products at 100 mJ/cm^2 (central zone)	2.3 ± 0.4
$PDMS_{150}$	Laser ejected products at 150 mJ/cm^2	0.7 ± 0.1
$PDMS_{200}$	Laser ejected products at 200 mJ/cm^2	189 ± 28
$PDMS_{250}$	Laser ejected products at 250 mJ/cm^2	212 ± 33
$PDMS_{pl1}$	Soft plasma	3.8 ± 1.8
$PDMS_{pl2}$	Plasma RIE	40.5 ± 3.2
$PDMS_l$	Liquid toluene	56.3 ± 5.1

3 Experimental results

The AFM image of the as-deposited reference PDMS polymer film (bare PDMS sample) and the corresponding optical image is shown in Fig. 1a, b, respectively. As concerns the MAPLE-treated samples ($PDMS_{60}$, $PDMS_{100}$, $PDMS_{150}$, $PDMS_{200}$ and $PDMS_{250}$), Fig. 1c–e, i–k depict the morphological effects after exposure to the toluene MAPLE-products at the different laser fluences and Fig. 1f–h, l–n are the corresponding AFM optical images.

In Table 1, a list of the samples, their preparation method and RMS surface roughness values are reported.

Exposition of the PDMS sample to the products ejected after laser irradiation of frozen toluene at $F = 60$ mJ/cm^2 has the effect to (1) induce a more opaque look of the sample at the naked-eye inspection, (2) create structures weakly visible by optical inspection (Fig. 1f), (3) increase the RMS surface roughness from (6.1 ± 0.8) nm to (53 ± 3) nm and (4) change the surface morphology too (see Fig. 1c, $PDMS_{60}$ sample, and compare it with Fig. 1a, b). In this respect, wrinkled structures began to be discerned. The behavior of the polymer film seems very different when the toluene target is irradiated at $F = 100$ mJ/cm^2. First of all, only in this case, two different zones can be distinguished on the PDMS surface: a central zone (Fig. 1d, g, $PDMS_{100a}$ sample) and a peripheral one (Fig. 1e, h, $PDMS_{100b}$ sample). In Table 1, such zones are referred to as zone (a) and zone (b), respectively. The central PDMS zone looks, at the naked-eye, very bright, showing some cracks, while the peripheral one looks more opaque. Optical

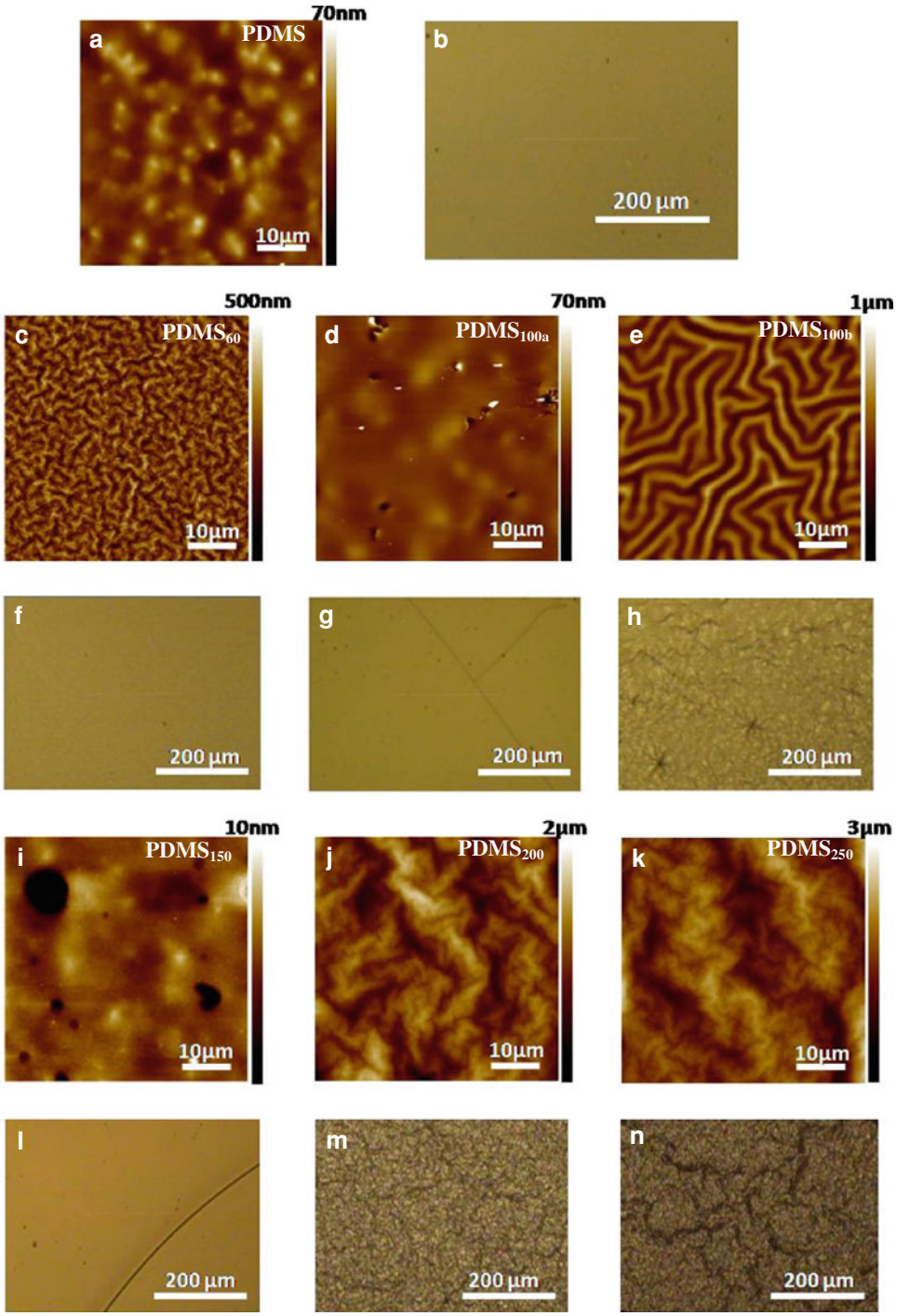

Fig. 1 AFM and optical images, respectively, of the **a** and **b** unexposed PDMS, **c** and **f** $PDMS_{60}$, **d** and **g** $PDMS_{100a}$, **e** and **h** $PDMS_{100b}$, **i** and **l** $PDMS_{150}$, **j** and **m** $PDMS_{200}$ and **k** and **n** $PDMS_{250}$ samples

inspection confirms the presence of cracks in zone (a) (Fig. 1g) and of structures in zone (b) (Fig. 1h). These differences correspond to different morphologies and RMS roughness values. AFM inspection shows that the bright region has a morphology similar to the as-deposited sample, but with a lower RMS roughness value (2.3 ± 0.4) nm with respect to (6.1 ± 0.8) nm. Some voids are also visible. Wrinkles dominate the morphology of the peripheral zone in a more ordered way and with a larger periodicity with respect to what seen after target irradiation at $F = 60$ mJ/cm^2. In this part of the sample, the RMS roughness reaches the value of about (105 ± 14) nm.

The increase of the laser fluence to 150 mJ/cm^2 had the effect to increase the naked-eye brightness of the sample and to further smooth the surface roughness to (0.7 ± 0.1) nm, (Fig. 1i, l, $PDMS_{150}$ sample), although more cracks were detected by optical inspection (Fig. 1l, $PDMS_{150}$ sample). The surface morphology of the samples

exposed to the ejected products obtained increasing the laser fluences to $F = 200$ and 250 mJ/cm^2 had both a wrinkled aspect in the AFM images as well as in the optical ones (Fig. 1j, m corresponding to the sample $PDMS_{200}$ and Fig. 1k, n, corresponding to the sample $PDMS_{250}$). The samples looked opaque and appeared rougher, too. As detailed in Table 1, very high roughness values were recorded in these cases: (189 ± 29) nm and (212 ± 33) nm, respectively. For comparison, in Fig. 2, the AFM and optical images of the PDMS film surface morphologies after different non-laser-based treatments are shown (Sect. 2.2). The corresponding roughness values are reported in Table 1 too.

It can be seen that the effect of saturated toluene vapors (Fig. 2a, b, $PDMS_v$ sample) and of the liquid toluene drop (Fig. 2c, d, $PDMS_l$ sample) is to increase the roughness

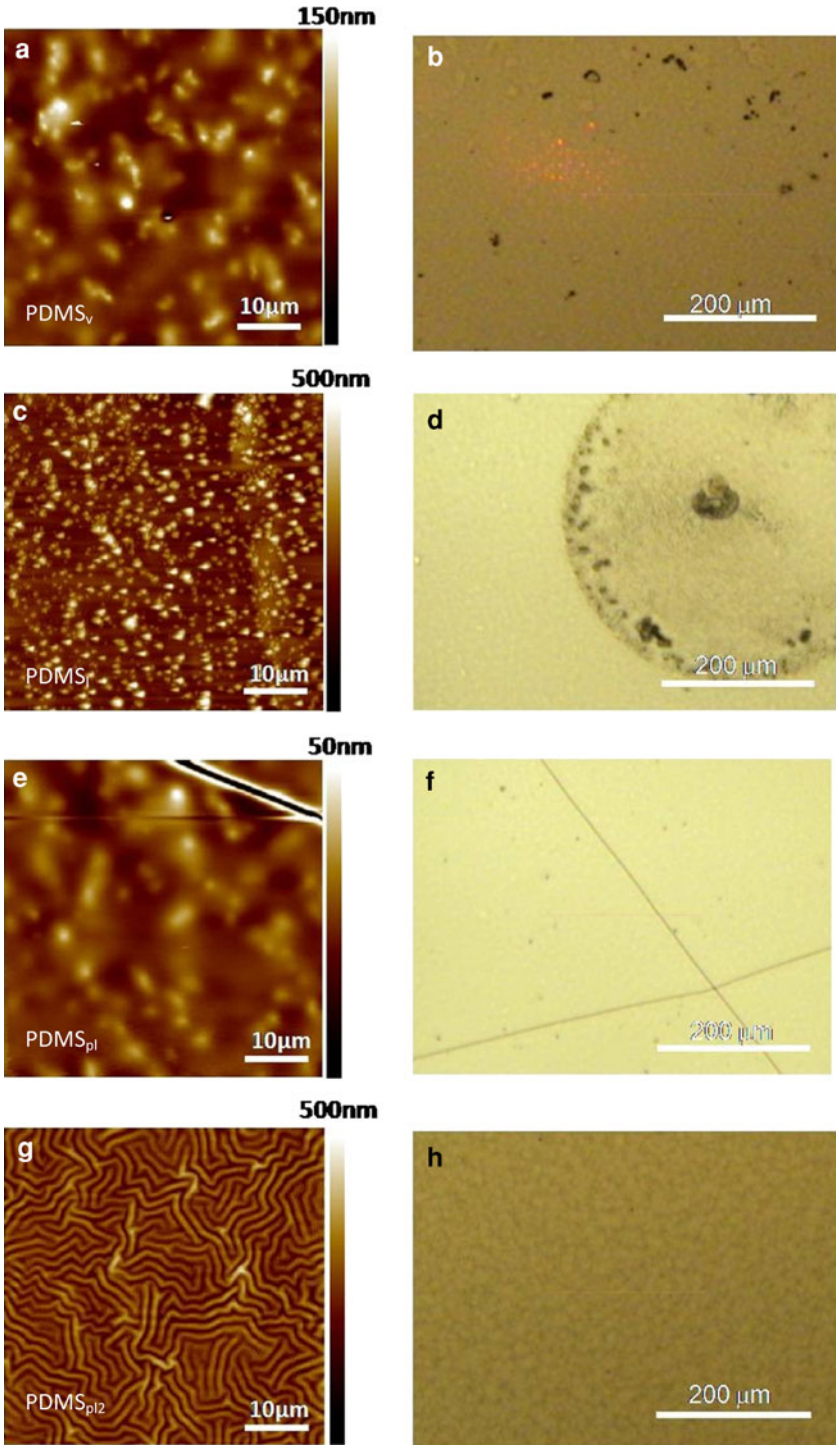

Fig. 2 AFM and optical images, respectively, of the **a** and **b** $PDMS_v$, **c** and **d** $PDMS_l$, **e** and **f** $PDMS_{pl1}$, **g** and **h** $PDMS_{pl2}$ samples

Table 2 Water contact angle values measured for the as-deposited PDMS polymer, PDMS exposed to toluene saturated vapors ($PDMS_v$), PDMS exposed to the ejection products after toluene irradiations ($PDMS_{60}$, $PDMS_{100}$, $PDMS_{150}$, $PDMS_{200}$ and $PDMS_{250}$) and PDMS exposed to oxygen plasma ($PDMS_{pl1}$ and $PDMS_{pl2}$)

Sample treatment	Contact angle (°)	RMS (nm)
PDMS	126.7 ± 2.2	6.1 ± 0.8
$PDMS_{60}$	71.3 ± 1.0	53 ± 3
$PDMS_{100}$	74.8 ± 0.6	2.3 ± 0.4
$PDMS_{150}$	68.5 ± 3.0	0.7 ± 0.1
$PDMS_{200}$	70.0 ± 0.5	189 ± 28
$PDMS_{250}$	74.6 ± 2.2	212 ± 33
$PDMS_{pl1}$	25 ± 3	3.8 ± 1.8
$PDMS_{pl2}$	≤10	40.5 ± 3.2

The contact angle values are compared with the RMS values reported in the second column extrapolated from AFM images of Figs. 1 and 2

value of the PDMS sample with respect to the as-deposited sample to (12.3 ± 1.5) nm and to (56.3 ± 5.1) nm, respectively. Optically, the samples appear more dirty and rough in the treated areas (see Fig. 2b, d). No wrinkled structures were observed. The same behavior was found after performing a soft treatment in oxygen plasma (RMS roughness value of (3.8 ± 1.8) nm, $PDMS_{pl1}$ sample) although, in this case, some cracks are present on the sample surface, as optical and AFM images show (Fig. 2e, f). It is noteworthy that in this case, the roughness value is lower with respect to the as-deposited PDMS sample. The situation is completely different when the PDMS film is treated with an oxygen plasma at higher power ($PDMS_{pl2}$ sample). In this case, wrinkled structures appeared on the sample surface, RMS roughness values of (40.5 ± 3.2) nm were recorded and no cracks were observed (see AFM images and optical images in Fig. 2g, h).

Contact angle (CA) measurements were performed on the as-deposited PDMS sample and on the treated ones. The results are reported in Table 2 and compared with the measured roughness values. As can be seen from this table, the effect of all the irradiation treatments was to increase the hydrophilicity of the PDMS film surfaces. In fact, the CA of the as-deposited PDMS film resulted to be (126.7 ± 2.2)°. The value of this parameter was reduced to ~70° for samples exposed to the products of toluene laser irradiation, almost independently on the laser fluences values. Samples exposed to oxygen plasma (samples $PDMS_{pl1}$ and $PDMS_{pl2}$) are extremely hydrophilic, due to the introduction of hydroxyl groups on the surface [37, 38].

4 Discussion

Assuming that there is no direct irradiation of the MAPLE-treated PDMS samples and the radiation diffused by the target surface is almost totally absorbed by the laser-removed material in front of the irradiated target (plume shielding effect), we suppose that no photo-oxidation due to the laser source is expected [39, 40]. Hence, the observed modifications of the PDMS sensing surfaces, in the performed test experiments, could be attributed to the interaction between the substrate and the residual solvent in front of the substrate. Under a practical point of view, it is important to understand in which form the solvent reaches the sensing material and how it may potentially affect the morphology and other properties of the growing MAPLE films. Since the birth of the MAPLE technique, it was recognized that the solvent plays a fundamental role as a "driving motor" of both ablation process and transport of the solute toward substrate. But, at first, a complete evacuation of the solvent vapors in the vacuum chamber was assumed. It means that the solvent should not influence the solute material film growth. However, the results of molecular dynamic simulations of the MAPLE process [34], performed to explain the rough surface morphology presented by most of the MAPLE-deposited films, suggested a completely different picture of the process. It was shown that it is an explosive process, very similar to PLD far from equilibrium conditions, leading to a prompt ejection of liquid droplets and small clusters of matrix-polymer structures, as well as of matrix molecules. Since formation of matrix-polymer structures also depends on the physical parameters of solvent and solute and on their interaction on short-range, the ejection of solvent droplets is strictly related to the ablation process, as well as to solvent volatility. In this respect, the basic question is about the ejected liquid droplets and matrix molecule. That is, are, in general, the droplets evaporated before their arrival on the substrate, as indicated by molecular dynamic simulations of the MAPLE process? Moreover, are the solvent molecules completely pumped away during the time of flight between the target and substrate?. In other words, although the MAPLE technique is a solvent-based technique, can it be considered a dry, or a wet process or a semidry process? The wide range of experimental parameters that can characterize a MAPLE deposition involves that very likely a fully general conclusion is not possible. Even if results depend on the experimental MAPLE parameters, the ideal picture (solvent-free deposits) of the MAPLE mechanism must be compared with the most usually occurring experimental conditions. In this spirit, the key point is to understand whether the solvent plays an active role in affecting the growing film besides being a solute vector from target to substrate.

In this study, the role of the solvent after its ejection from the frozen condensed phase was considered and investigated. The reason underlying our choice of using a target formed by only the frozen solvent was based on the

inherent principle of the MAPLE technique. Indeed, it must be considered that the solvent represents most of the target composition (the solute represents only a few weight percent of the solution). Another important prerequisite for a successfully MAPLE experiment is to start from a homogeneous solvent/solute solution: the solvent must dissolve the solute [35].

With the aim of detecting any presence of the solvent at the substrate position, a reference soft polymer film (PDMS) sensitive to the used solvent, toluene [32], was placed in front of the target at the substrate position like in a conventional MAPLE experiment. In this respect, the set distance target substrate (6 cm) is large enough to allow one to suppose that a highly volatile solvent should be able to evaporate for the most part. Larger distance would cause a deposition rate too low for any practical use.

As concerns the laser fluence parameter, the starting value was chosen to be 60 mJ/cm^2, slightly above the threshold fluence [36], to have material ejection in a MAPLE process, and not a purely evaporative process without polymer ejection [34].

Looking at the AFM (Fig. 1c) and optical images (Fig. 1f) of the $PDMS_{60}$ sample exposed to the material ejected after toluene irradiation at the lowest fluence value considered in this study (60 mJ/cm^2), some solvent-induced effects are evident on the PDMS film placed at the substrate position since a very different surface morphology appears as compared to the untreated PDMS film (Fig. 1a, b). This finding suggests that, even just above the ablation fluence threshold, solvent might influence the polymer morphology. From a comparison between the structures of the PDMS samples exposed to saturated toluene vapors ($PDMS_v$ sample, Fig. 2a, b) and to a drop of toluene ($PDMS_l$ sample, Fig. 2c, d), it seems that upon laser irradiation at 60 mJ/cm^2, toluene does not arrive on the sample in the form of droplets or "thermal vapors," since their effect on PDMS samples was only to change the surface roughness, without inducing any patterning of the surface. We can suppose that toluene reaches the surface in the form of "energetic" vapor molecules "bombarding" the sample surface, thus inducing the formation of wrinkled structures due to the relaxation of thermally or mechanically induced compressive stress [37].

Breaking of the toluene molecules, by photochemical effects, is possible at the target position and/or in the gas phase, after its ejection from the condensed phase, since the energy of the C–C bond (the bond which in a toluene molecule, C_6H_5–CH_3, linksaryl and methyl groups) is reported to be 3.6 eV, while the photon energy of the ArF excimer laser used in our tests is 6.4 eV.

The formation of wrinkled structures in PDMS when exposed to oxygen plasma was already reported [37, 38, 41–44], as well as the formation of cracks [37, 38]. The presence of wrinkled structures, in the peripheral zone of the $PDMS_{100}$ sample (Fig. 1e), exposed to the toluene irradiation products at the fluence of 100 mJ/cm^2, which are very similar to those obtained after RIE plasma exposure ($PDMS_{pl2}$ sample Fig. 2g, optical images in Fig. 2h), reinforces the hypothesis of plasma formation already at this low fluence values. The absence of wrinkles in the central zone of this sample and of the sample exposed to the toluene irradiation products at $F = 150$ mJ/cm^2 could be due to a film relaxation induced by the cracks formation (see Fig. 1i, l). It is important to stress, at this point, that a lower surface roughness in connection with the crack presence was also observed for the film exposed to a soft oxygen plasma ($PDMS_{pl1}$ sample, Fig. 2e, f to be compared with Fig. 1i, l, for example). Irradiation of the toluene target with fluence values of 200 and 250 mJ/cm^2 has a more deleterious and deep effect on the PDMS sample morphology, which is not easily recovered by the elastic properties of the polymer itself.

The occurrence of two zones with different features observed only for the sample $PDMS_{100}$ can be explained based on the laser fluence used range and the different relaxation mechanism involved for the polymer films. It is well known that, after oxygen plasma irradiation, a more hydrophilic, hard layer is formed on the PDMS upper layers [37]. The stiffness and thickness of the formed layer is related to the chemical composition and the fluence of the plasma, which determine the formation of a superficial layer with properties very different from those of the bulk PDMS; the consequent mechanical stress drives several relaxation mechanisms, which cause cracks or wrinkled structures above an energetic threshold. Accounting for all this, an energetic threshold is expected, which determines whether MAPLE-treated PDMS samples may relax generating cracks or periodic arrangements. In a typical ablation process, the generated plume has a complex composition and expands driven by gradients of pressure, temperature and mass with its angular distribution becoming more strongly peaked for increasing energy of the ablation products. In absence of plume compression due to inert background gas, at low (just above the ablation threshold) fluence, the heaviest species propagate along the forward direction and the lightest peripheral species are more strongly diffused than the heaviest counterparts. In contrast, well above the threshold fluence, no significant selection mechanism occurs for the energetic plume components. Therefore, an exposure of the same PDMS sample to a MAPLE plume, generated just above the threshold ablation (namely with a lateral energy gradient, which does not necessarily mean a two-component plume), may allow visualizing different effects on the PDMS-exposed surface depending on the relaxation mechanisms involved by the plume energy distribution.

We believe that the fluence of 100 mJ/cm^2 (the toluene ablation threshold is 60 mJ/cm^2 [36]) represents a threshold value yielding different energy regimes in the impinging plasma plume (a less energetic peripheral one and a more energetic central one). This could be the reason why both the morphologies (corresponding to the two different relaxation mechanisms) are visualized on the same sample.

It is noteworthy that while upon oxygen plasma-treatment increasing fluence determines a transition from cracks to waves, the opposite occurs for toluene plasma streams. An explanation of this phenomenon on the basis of the present study would be too ambitious; however, we can only assess that toluene and oxygen are compounds very different under a compositional point of view and, consequently, the upper layer they generate in a plasma-like form as well as the heating effects they may induce are different.

At this level, the presented results strongly suggest that the MAPLE process could be considered a "semidry" process, in the sense that the ablated pure solvent could not be in general completely eliminated after the irradiation process during the fly phase. Notably, the solvent, if sufficiently volatile, like toluene in this case, is not present in liquid phase but in form of vapor molecules (neutral, ionized and probably dissociated).

Another proof that energetic toluene vapors reach the PDMS sensing surface may come from a comparison of the wettability properties of PDMS samples with similar roughness/morphology. In Table 2, the RMS and CA values are reported of all the investigated samples. It is clear that PDMS surfaces exhibiting only cracks (i.e. the samples PDMS$_{100}$, PDMS$_{150}$ and PDMS$_{pl1}$—see the associated optical and AFM images in Figs. 1, 2) and with RMS and AFM morphology similar to untreated PDMS show different wettability. It is well known that the PDMS$_{pl1}$ sample is chemically functionalized after oxygen plasma treatments with –OH groups [37, 38]; therefore, the increased hydrophilicity of the samples PDMS$_{100}$ and PDMS$_{150}$ may be only ascribed to the addition of some groups (probably coming from ions/radicals generated by high energetic toluene vapors) that makes the resulting surface more hydrophilic.

Moreover, the comparison between the CAs of the samples PDMS$_{60}$ and PDMS$_{pl2}$ with similar wrinkled morphology and RMS confirms that, despite both samples relax in the same way after being stimulated with energetic vapors, they show different wettability, being probably functionalized with gas phases of different chemical nature (toluene for PDMS$_{60}$ and oxygen for PDMS$_{pl2}$).

These results support the idea that after the irradiation treatments (described in Sect. 2.1), the PDMS surface of the samples is derivatized with different (probably more hydrophilic) functional groups. Such groups may come from ionized species generated by plasma-like energetic toluene vapors.

5 Conclusions

In this study, the MAPLE process was investigated adopting a new point of view, based on the investigation of the effects of the laser-induced solvent vapors on the film-growing surface. The solvent ablation products were obtained by laser irradiation of a pure solvent frozen target. The presence of the solute in the actual MAPLE deposition should not dramatically change the scenario due to the very low solute concentration and basic MAPLE mechanism. Even if a slight decrease of the threshold fluence could occur in presence of solute, the observed effect of the solvent energetic vapors on the growing film should still occur because MAPLE depositions operate above the fluence threshold to assure an efficient deposition rate.

From the results obtained in this study and under the considered experimental conditions, it appears that the MAPLE process cannot be considered a purely dry process, as originally proposed. It should be considered, more correctly, a "semidry" process in the sense that the solvent could be generally not completely evacuated during its landing from the laser-irradiated frozen target to the substrate. The solvent, if sufficiently volatile, is not present in liquid phase at the substrate position, but in form of vapor molecules (neutral, ionized and possibly dissociated). Comparison with other plasma-based treatments shows that laser-induced plasma formation possibly starts at the laser fluences conventionally used in MAPLE experiments, thus influencing morphology and chemistry as well as superficial wettability of the growing film. This evidence is particularly important for MAPLE depositions of soft materials and polymeric bilayers.

Acknowledgments The authors thank A. Luches for helpful discussion and suggestions.

References

1. B. Cho, S. Song, Y. Ji, T.-W. Kim, T. Lee, Adv. Funct. Mater. **21**, 2806 (2011)
2. H. Sirringhaus, Adv. Mater. **17**, 2411 (2005)
3. J. Shinar, R. Shinar, J. Phys. D Appl. Phys. **41**, 133001 (2008)
4. G. Witte, C. Wöll, J. Mater. Res. **19**, 1889 (2004)
5. Y. Fujii, H. Atarashii, M. Hino, T. Nagamura, K. Tanaka, Appl. Mater. Interfaces **1**, 1856 (2009)
6. A.L. Layzner, C.J. Tassone, S.H. Tolbert, B.J. Schwartz, J. Phys. Chem. C **113**, 20050 (2009)
7. X. Zhang, J.F. Douglas, R.L. Jones, Soft Matter, Mar. 21, (2012). doi:10.1039/C2SM07308K

8. R. Srinivasan, V. Mayne-Banton, Appl. Phys. Lett. **41**, 576 (1982)
9. Y. Kawamura, K. Toyoda, S. Namba, Appl. Phys. Lett. **40**, 374 (1982)
10. R. Srinivasan, B. Braren, Chem. Rev. **89**, 1303 (1989)
11. D. Bauerle, *Laser Processing and Chemistry*, 3rd edn. (Springer, Berlin, 2000)
12. S. Lazare, V. Granier, Laser Chem. **10**, 25 (1989)
13. T. Lippert, J.T. Dickinson, Chem. Rev. **103**, 453 (2003)
14. T. Lippert, in *Polymers and Light*, vol. 168, ed. by T. Lippert (Springer, Berlin, 2004), p. 51
15. P.E. Dyer, in *Photochemical Processing of Electronic Materials*, ed. by I.W. Boyd, R.B. Jackman (Academic, London, 1992), p. 360
16. N. Bityurin, B.S. Luk'yanchuk, M.H. Hong, T.C. Chong, Chem. Rev. **103**, 519 (2003)
17. T. Lippert, Plasma Process. Polym. **2**, 525 (2005)
18. N. Bityurin, Annu. Rep. Progr. Chem. C **101**, 216 (2005)
19. D.B. Chrisey, A. Pique, R.A. McGill, J.S. Horwitz, B.R. Ringeisen, D.M. Bubb, P.K. Wu, Chem. Rev. **103**, 553 (2003)
20. A. Piqué, P.K. Wu, B.R. Ringeisen, D.M. Bubb, J.S. Melinger, R.A. McGill, D.B. Chrisey, Appl. Surf. Sci. **186**, 408 (2002)
21. A.P. Caricato, M. Lomascolo, A. Luches, F. Mandoj, M.G. Manera, M. Mastroianni, M. Martino et al., Appl. Phys. A Mater. Sci. Process. **93**, 651 (2008)
22. A. Stanculescu, L. Vacareanu, M. Grigoras, M. Socol, G. Socol, F. Stanculescu, N. Preda, Appl. Surf. Sci. **257**, 5298 (2011)
23. B.R. Ringeisen, J. Callahan, P.K. Wu, A. Piqué, B. Spargo, R.A. McGill, M. Bucaro, H. Kim, D.M. Bubb, D.B. Chrisey, Langmuir **17**, 3472 (2001)
24. I.A. Paun, V. Ion, A. Moldovan, M. Dinescu, App. Phys. Lett. **96**, 243702 (2010)
25. C.S. Ciobanu, S.L. Iconaru, E. Gyorgy, M. Radu, M. Costache, A. Dinischiotu, P. Le Coustumer, K. Lafdi, D. Predoi, Chem. Cent. J. **6**, 17 (2012)
26. Y. Guo, A. Morozov, D. Schneider, J.W. Chung, C. Zhang, M. Waldmann, N. Yao, G. Fytas, C.B. Arnold, R.D. Priestley, Nat. Mater. **11**, 337 (2012)
27. T.M. Patz, A. Doraiswamy, R.J. Narayan, N. Menegazzo, C. Kranz, B. Mizaikoff, Y. Zhong, R. Bellamkonda, J.D. Bumgardner, S.H. Elder, X.F. Walboomers, R. Modi, D.B. Chrisey, Mater. Sci. Eng. C **27**, 514 (2007)
28. V. Califano, F. Bloisi, L.R.M. Vicari, P. Colombi, E. Bontempi, L.E. Depero, Appl. Surf. Sci. **254**, 7143 (2008)
29. A. Stanculescu, M. Socol, G. Socol, I.N. Mihailescu, M. Girtan, F. Stanculescu, Appl. Phys. A **104**, 921 (2011)
30. N.B. Ukah, D. Adil, J. Granstrom, R.K. Gupta, K. Ghosh, S. Guha, Org. Electron. **12**, 1580 (2011)
31. A.P. Caricato, M. Cesaria, G. Gigli, A. Loiudice, A. Luches, M. Martino, V. Resta, A. Rizzo, A. Taurino, Appl. Phys. Lett. **100**, 073306 (2012)
32. J.N. Lee, C. Park, G.M. Whitesides, Anal. Chem. **75**, 6544 (2003)
33. J. Hermann, A.L. Thomann, C. Boulmer-Leborgne, B. Dubreuil, M.L. De Giorgi, A. Perrone, A. Luches, I.N. Mihailescu, J. Appl. Phys. **77**, 2928 (1995)
34. E. Leveugle, L.V. Zhigilei, J. Appl. Phys. **102**, 074914 (2007)
35. A.P. Caricato, A. Vantaggiato, D. Valerini, A. Cretì, M. Lomascolo, M.G. Manera, R. Rella, M. Anni, G. Leggieri, M. Martino, Appl. Phys. A **101**, 759–764 (2010)
36. O. Kokkinaki, S. Georgiou, Dig. J. Nanomater. Biostruct. **2**, 221 (2007)
37. N. Bowden, W.T.S. Huck, K.E. Paul, G.M. Whitesides, Appl. Phys. Lett. **75**, 2557 (1999)
38. V. Arima, M. Bianco, A. Zacheo, A. Zizzari, E. Perrone, L. Marra, R. Rinaldi, Thin Solid Films **520**, 2293 (2012)
39. K. Rubahn, J. Ihlemann, G. Jakopic, A.C. Simonsen, H.-G. Rubahn, Appl. Phys. A **79**, 1715–1719 (2004)
40. N. Ikeda, N. Nakashima, K. Yoshihara, J. Chem. Phys. **82**, 5285 (1985)
41. K. Tsougeni, G. Boulousis, E. Gogolides, A. Tserepi, Microelectron. Eng. **85**, 1233 (2008)
42. K. Tsougeni, A. Tserepi, G. Boulousis, V. Constantoudis, E. Gogolides, Jpn. J. Appl. Phys. **46**, 744 (2007)
43. K. Tsougeni, A. Tserepi, G. Boulousis, V. Constantoudis, E. Gogolides, Plasma Process. Polym. **4**, 398 (2007)
44. A. Tserepi, E. Gogolides, K. Tsougeni, V. Constantoudis, E.S. Valamontes, J. Appl. Phys. **98**, 113502 (2005)